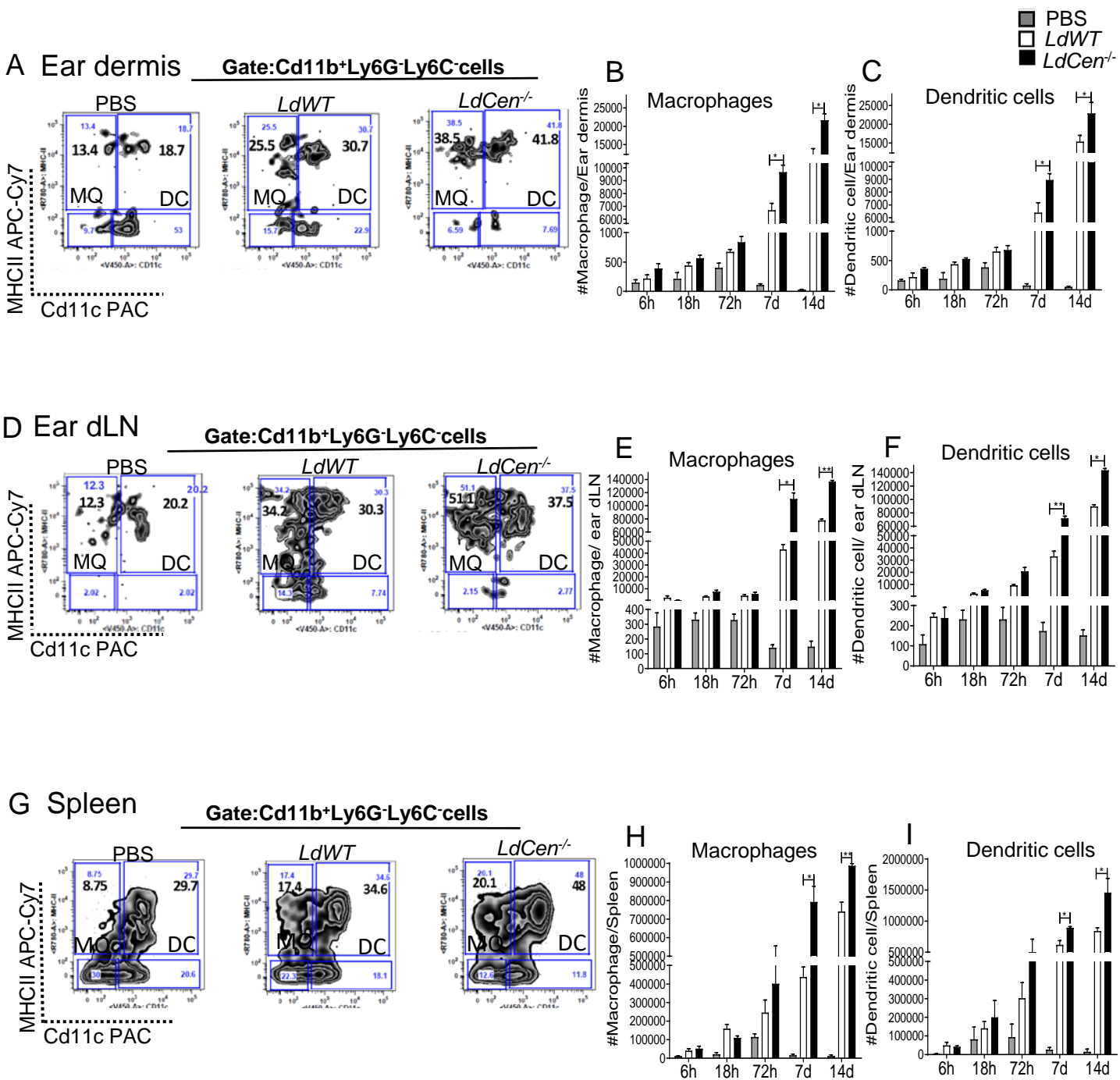
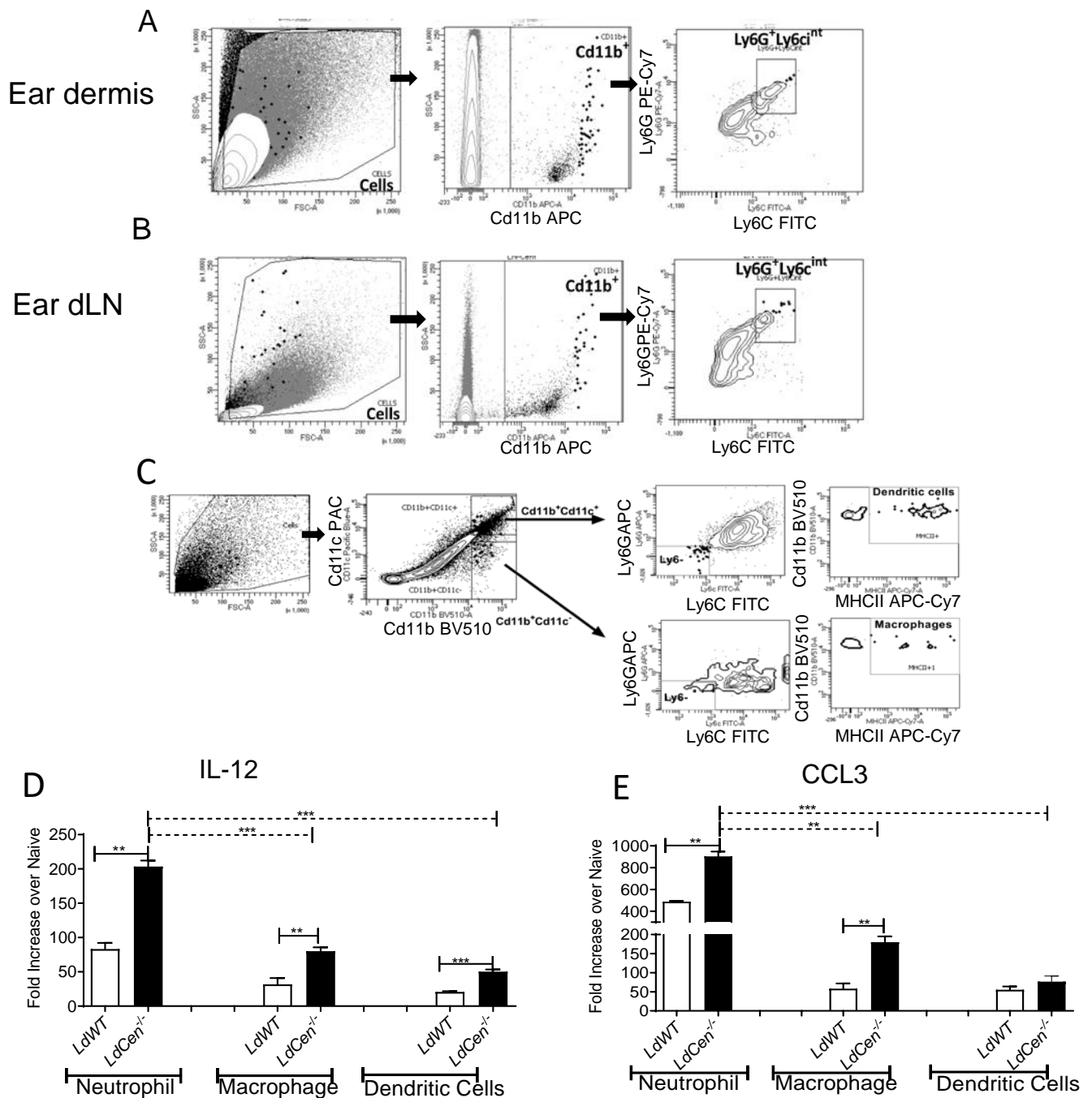


Supplementary Fig 1: Kinetics of neutrophil recruitment following *LdCen*^{-/-} intradermal infection. The gating strategy and individual flow plots for neutrophil $\text{Cd11b}^+\text{Ly6G}^+\text{Ly6c}^{\text{int}}$ recruitment in (A) ear dermis, (C) ear dLN and (D) spleen are shown for a specific significant time point. (B) Individual flow plots showing the changes in the subsets of $\text{RFP}^+/\text{mCherry}^+$ neutrophils in ear dermis recovered 6h post infection. (NP=Neutrophil) (n=6)

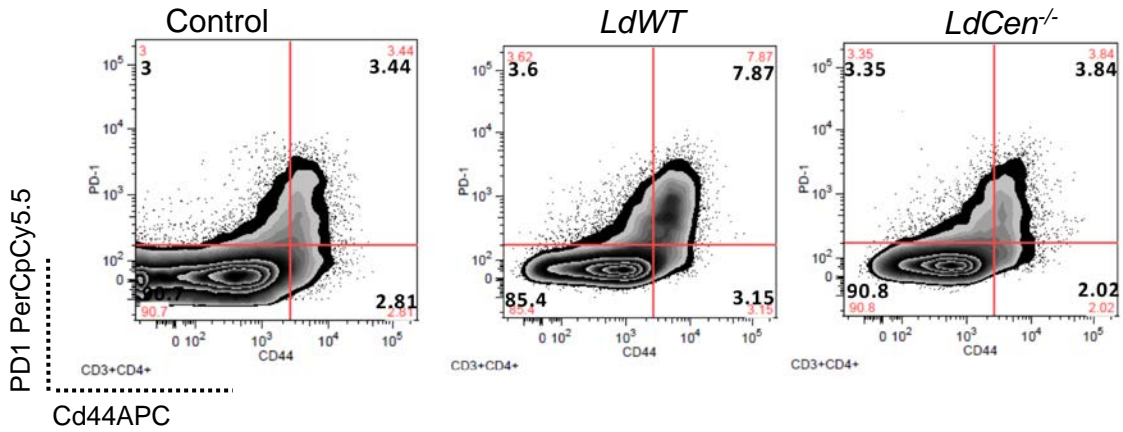


Supplementary Fig 2: Kinetics of myeloid cell recruitment following *LdCen*^{-/-} intradermal infection The gating strategy and individual flow plots for macrophages (Cd11b⁺Ly6G⁻Ly6C⁻CD11c⁻MHCII⁺) and DCs (Ly6G⁻Ly6C⁻CD11c⁺MHCII⁺) recruitment in (A) ear dermis, (D) ear dLN and (G) spleen are shown for a specific significant time point. Changes in the total number of MQ and DCs (B, C) per ear dermis (E, F) ear dLN and (H, I) spleen. Values shown are the mean numbers of cells per ear/ dLN and spleen ± standard deviations of results. 6–8 ears, dLN and spleen at each time point, pooled data from 3 independent experiments (n=6). * P < 0.05; ** P < 0.005.

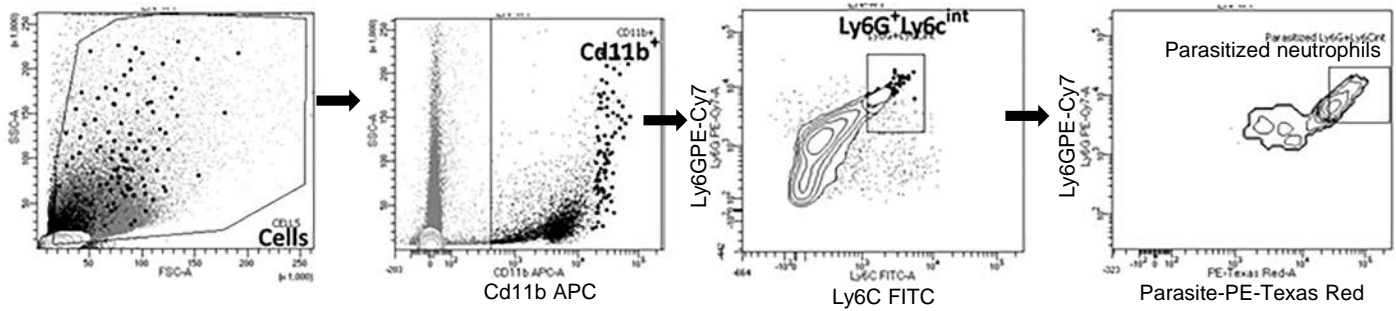


Supplementary Fig 3: *LdCen*^{-/-} intradermal infection induced significantly higher pro-inflammatory neutrophils (A, B) Neutrophils (*Cd11b*⁺*Ly6G*⁺*Ly6C*^{int}) were flow sorted from the ear dermis and ear dLN 18h and 72h post infection. The sorting strategy has been displayed in (A) ear dermis and (B) ear dLN. (n=6). (C) Macrophages (*Cd11b*⁺*Ly6G*⁺*Ly6C*⁺*Cd11c*⁻*MHCII*⁺) and DCs (*Cd11b*⁺*Ly6G*⁺*Ly6C*⁻*Cd11c*⁺*MHCII*⁺) were flow sorted from the ear dLN 48h post infection. The sorting strategy has been displayed. (n=6) (D, E) Cytokine and chemokine mRNA expression in ear dLN by neutrophil, macrophages and DCs 48h post infection. The experiment was repeated 3 times with pooled digests from 6-8 ear dLN per experiment. The data represent the mean values \pm standard deviations of results from 3 independent experiments that all yielded similar results (n=6). ** $P < 0.005$, * $P < 0.0005$.**

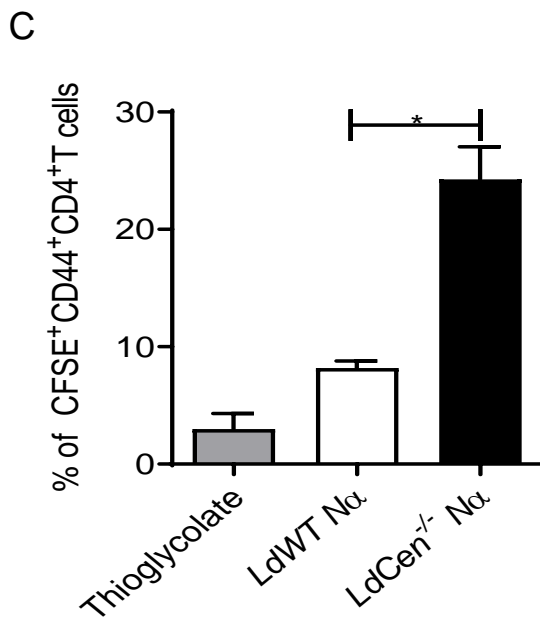
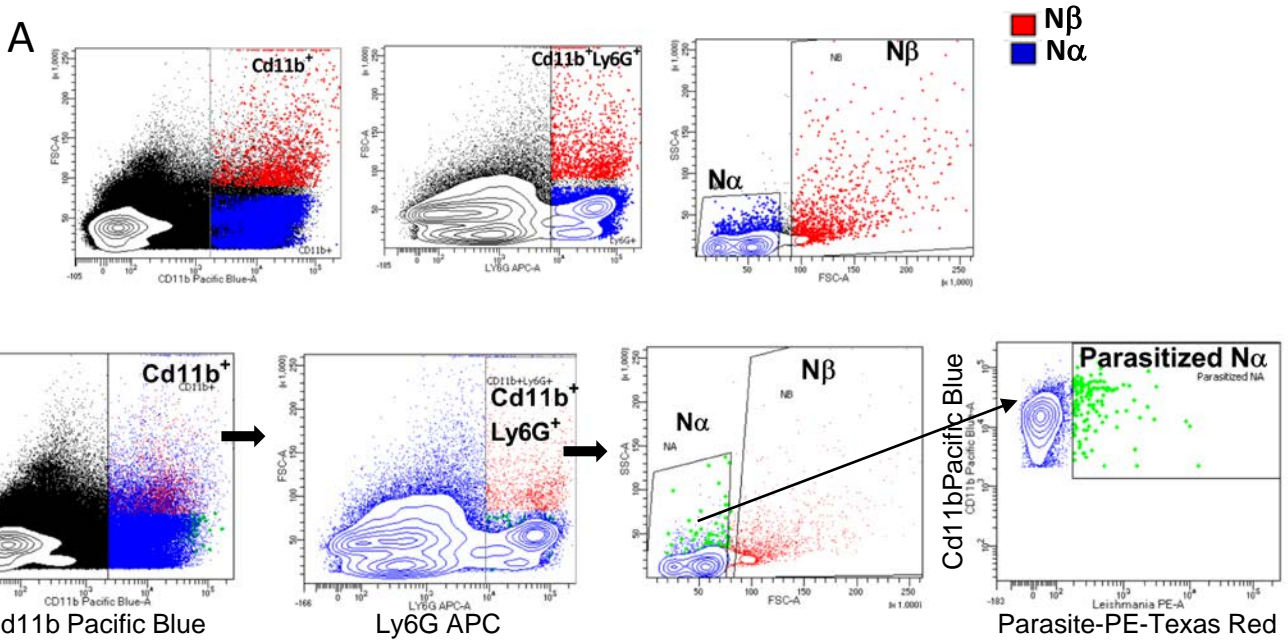
A Gate: CD3⁺CD4⁺ cells



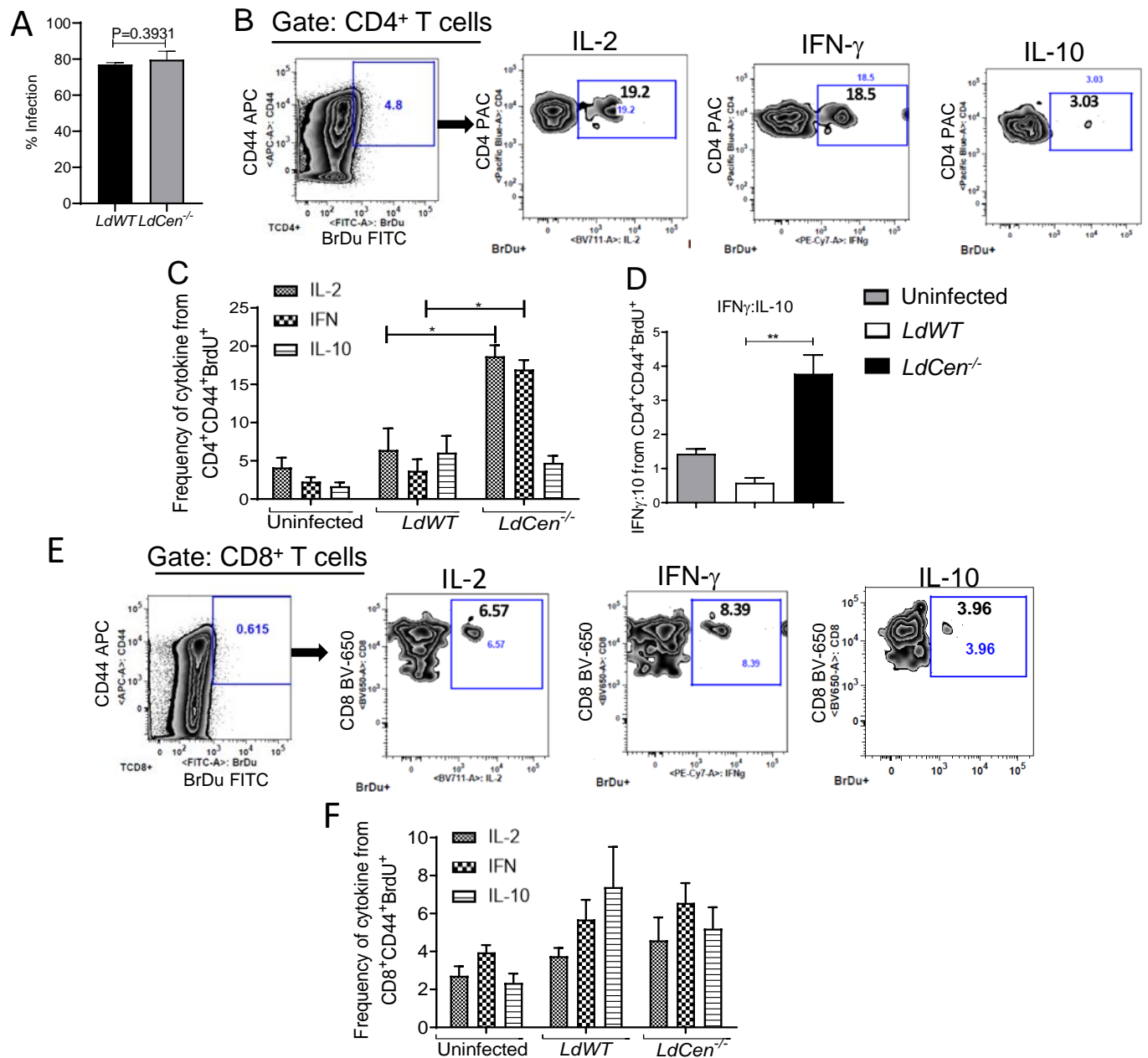
B



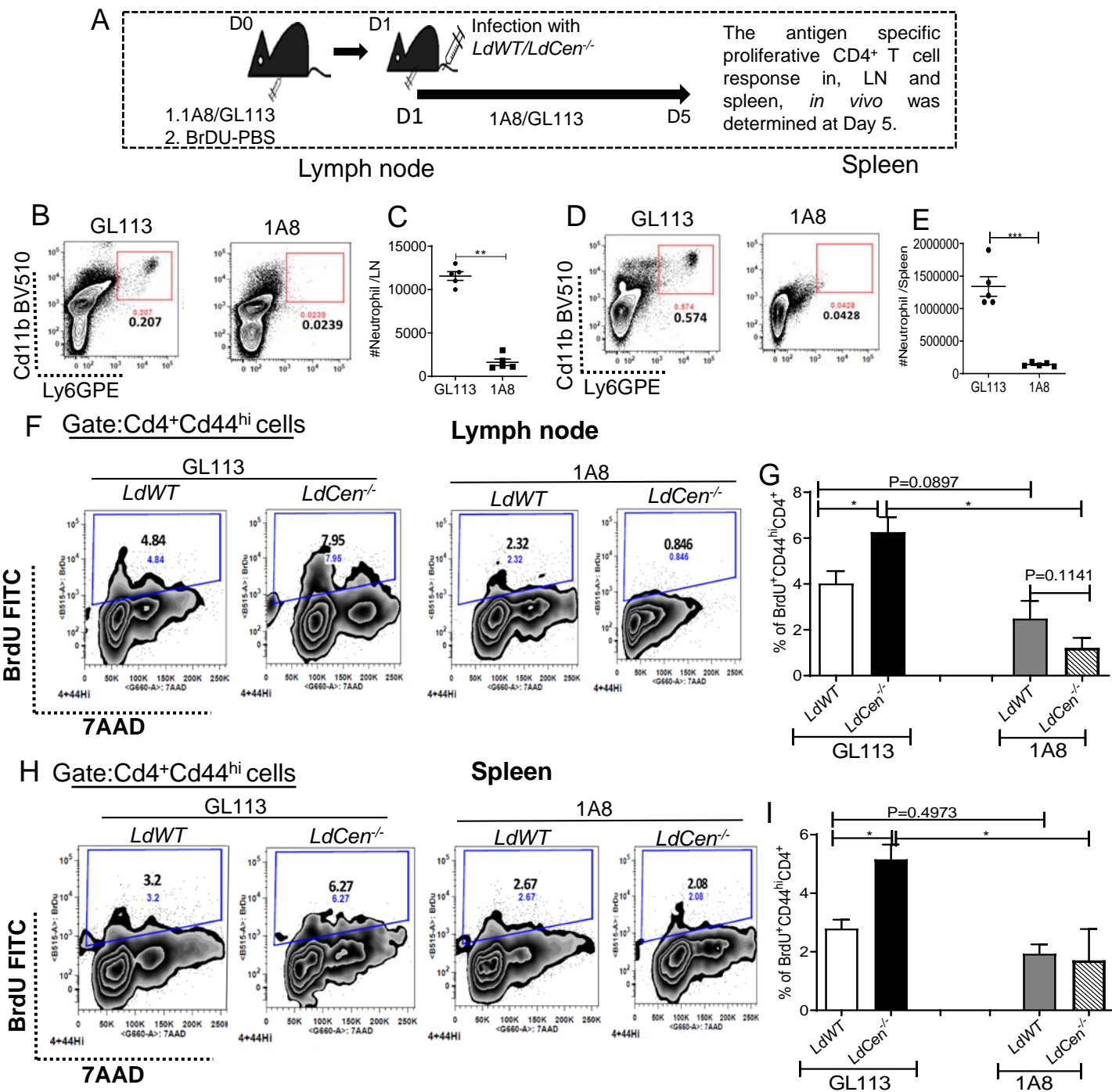
Supplementary Fig 4: PD-1 expression on antigen specific CD4⁺T cells from ear dLN of LdWT and LdCen^{-/-} infected mice: (A) Percentages of antigen specific CD4⁺T cells (CD4⁺CD44⁺) in ear dLN expressing PD-1 as measured by flow cytometry and the gating strategy and representative flow plots have been shown. (n=4). (B) Sorting strategy showing parasitized neutrophils isolation from ear dLN: Mice (n=6) were injected with PBS or LdWT^{RFP} or LdCen^{-/-mCherry} parasites. Parasitized neutrophils (Cd11b⁺Ly6G⁺Ly6C^{int}RFP/mCherry⁺) were flow sorted from the ear dLN 48h post infection.



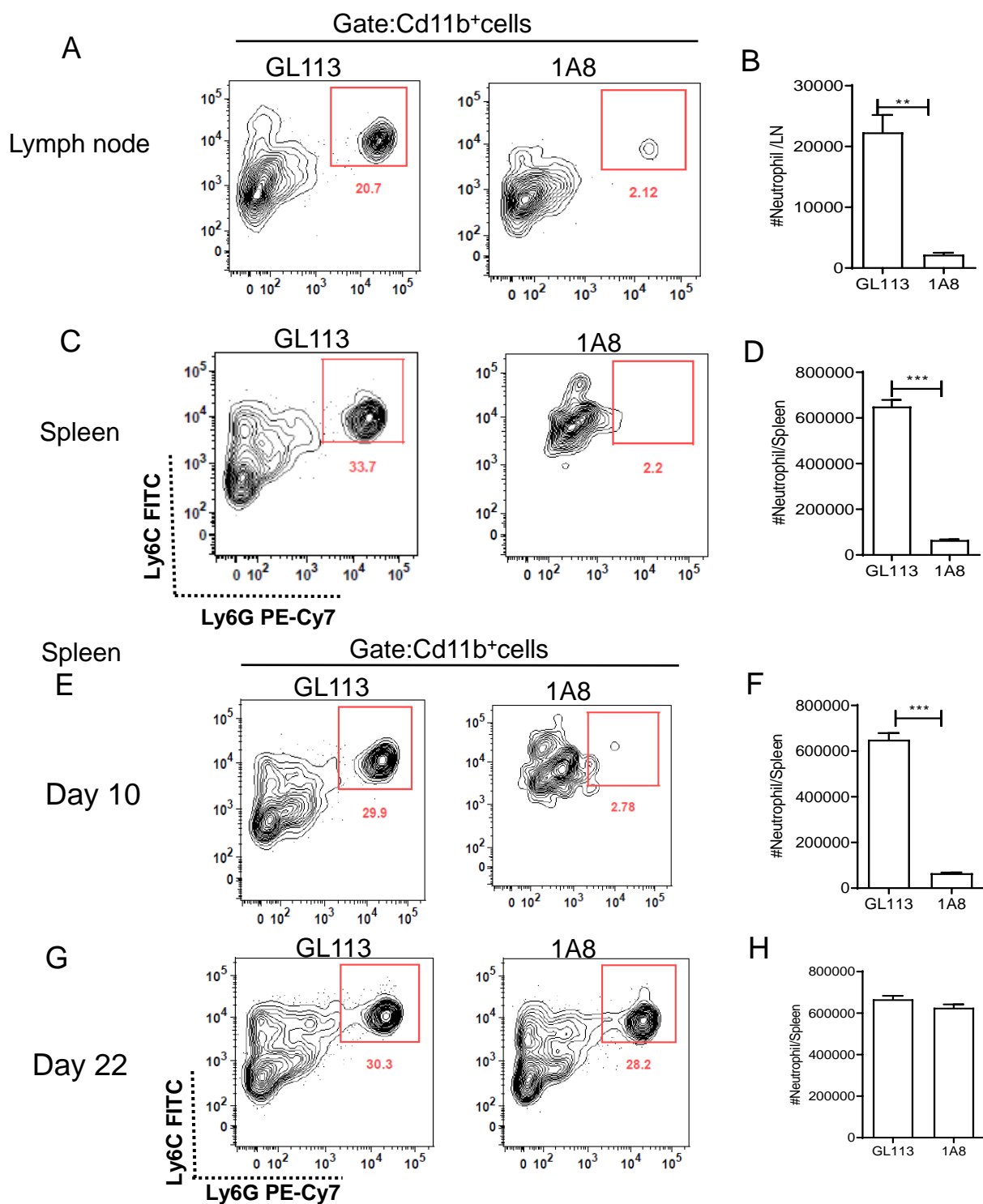
Supplementary Fig 5: Sort selection of $N\alpha$ neutrophils and CD4 T cell proliferation assay. (A) $N\alpha$ population from uninfected, LdWT and LdCen^{-/-} infected mice (n=6) ear dLN were flow sorted and the representative sorting strategy has been displayed. (B) Parasitized $N\alpha$ population from LdWT and LdCen^{-/-} infected mice (n=6) ear dLN were flow sorted and the representative sorting strategy has been displayed. (C) The bar diagram represents % cell showing CFSE dilution on gated CD4⁺CD44^{hi} cells. Cell proliferation was analyzed in triplicate experiments. * P < 0.05



Supplementary Fig 6: Adoptive transfer of LdCen^{-/-} parasite bearing neutrophil induced heightened antigen specific lymph node CD4⁺Th1 cell proliferation in vivo compared to LdWT. (A) Percent infection in the neutrophils following fluorescent LdWT/ LdCen^{-/-} infection (1:15 cell: parasite) in vitro. Graphs show mean \pm standard deviations of results from 3 independent experiments that all yielded similar results. (B) The gating strategy and representative flow plots for cytokine secreting CD44⁺BrdU⁺CD4⁺ T cells are shown. (C) The bar diagram represents CD44⁺BrdU⁺IL-2, IFN γ or IL-10 producing CD4⁺Th1 cells and (D) The IFN γ :IL-10 ratio was calculated from the data shown in (C). (E) The gating strategy and representative flow plots for cytokine secreting CD44⁺BrdU⁺CD8⁺ T cells are shown. (F) CD44⁺BrdU⁺IL-2, IFN γ or IL-10 producing CD8⁺T cells. The data represent the mean values \pm SD of results from 3 independent experiments (n=6). * P < 0.05; **P < 0.005.



Supplementary Fig 7: Depletion of neutrophil significantly abrogates *LdCen^{-/-}* induced CD4⁺T cell proliferation *in vivo*. (A) Schematic diagram showing experimental scheme for neutrophil depletion and BrdU staining. (B, C, D, E) Representative plot showing mean total number of neutrophils per lymph node and spleen on day 5 in the GL113 or 1A8 treated mice. \pm SEM of results from two independent experiments. Mean and SEM of 5 mice in each group are shown ** $P < 0.005$; *** $P < 0.0005$. (F, H) The gating strategy for the proliferation of lymph nodes and spleen BrdU⁺CD44⁺CD4⁺T cells are shown under GL113 and 1A8 treatment. (G, I) The bar diagram represent percentage of BrdU⁺CD44⁺CD4⁺T cells in the lymph node and spleen. The data represent the mean values \pm SEM of results from two independent experiments ($n=6$). * $P < 0.05$.



Supplementary Fig 8: Checking the depletion efficiency of 1A8 for neutrophils in lymph node and spleen
 (A, B, C, D) Representative dot plots and mean total number of neutrophils (Cd11b⁺Ly6G⁺Ly6C^{int}) in the GL113 or 1A8 treated mice lymph nodes and spleen. (E) Representative dot plots and (F) mean total number of neutrophils per spleen of GL113 or 1A8 treated mice 10 days after neutrophil depletion. (G) Representative dot plots and (H) mean total number of neutrophils per spleen of GL113 or 1A8 treated mice after subsequent repletion till day 22. \pm SEM of results from 2 independent experiments. Mean and SEM of 3 mice in each group are shown. ** $P < 0.005$; *** $P < 0.0005$.